Author(s): Polity, A. & Krause-Rehberg, R. & Staab, T. E. M. & Puska, Martti J. & Klais, J. & Möller, H. J. & Meyer, B. K.

Title: Study of defects in electron irradiated CuInSe[sub 2] by positron lifetime spectroscopy

Year: 2016

Version: Final published version

Please cite the original version:

Polity, A. & Krause-Rehberg, R. & Staab, T. E. M. & Puska, Martti J. & Klais, J. & Möller, H. J. & Meyer, B. K. 2016. Study of defects in electron irradiated CuInSe[sub 2] by positron lifetime spectroscopy. Journal of Applied Physics. Volume 83, Issue 1. 71-78. ISSN 0021-8979 (printed). DOI: 10.1063/1.366703.

Study of defects in electron irradiated CuInSe 2 by positron lifetime spectroscopy

A. Polity, R. Krause-Rehberg, T. E. M. Staab, M. J. Puska, J. Klais, H. J. Möller, and B. K. Meyer

Citation: Journal of Applied Physics **83**, 71 (1998); doi: 10.1063/1.366703
View online: http://dx.doi.org/10.1063/1.366703
View Table of Contents: http://scitation.aip.org/content/aip/journal/jap/83/1?ver=pdfcov
Published by the AIP Publishing

Study of defects in electron irradiated $CuInSe_2$ by positron lifetime spectroscopy

A. Polity,[a] R. Krause-Rehberg, and T. E. M. Staab
Fachbereich Physik, Universität Halle, D-06099 Halle (Saale), Germany

M. J. Puska
Laboratory of Physics, Helsinki University of Technology, 02150 Espoo, Finland

J. Klais and H. J. Möller
Fachbereich Physik, Technische Universität Bergakademie Freiberg, D-09599 Freiberg, Germany

B. K. Meyer
Fachbereich Physik, Justus–Liebig–Universität Giessen, D-35392 Giessen, Germany

(Received 7 July 1997; accepted for publication 26 September 1997)

$CuInSe_2$ was studied in the as-grown state and after low-temperature (4 K) 2 MeV electron irradiation. The positron bulk lifetime of 235 ps was measured for the unirradiated sample. The positron bulk lifetime was theoretically calculated and is in good agreement with the experimental value. In addition, the defect-related lifetimes for mono-, di-, and trivacancies are theoretically determined. An increased average positron lifetime indicated after electron irradiation the appearance of open-volume defects, most probably of divacancy type. The disappearance of this defect was observed during annealing below 250 K. Other defects were formed leading to a divacancy signal at least stable up to 600 K in the temperature range above 450 K. © *1998 American Institute of Physics.* [S0021-8979(98)04101-2]

I. INTRODUCTION

The ternary I–III–VI_2 compounds, such as $CuInSe_2$ (CIS), crystallize in the chalcopyrite structure. CIS-based layers are used as very high-efficient adsorbers for thin-film solar cells. The best conversion efficiency experimentally observed is 17%.[1] A further important advantage of this material is the high radiation resistance.[2]

Point defects influence electrical and optical properties of CIS. Native defects partly compensate deviations from the ideal stoichiometry. Some of them introduce energy levels in the band gap and, therefore, the conductivity type can be adjusted by appropriate compositions of the compound. A difficulty is the large number of intrinsic defects in ternary compounds. Calculations of the defect chemistry of this compound, and also of other $A_aB_bX_c$ compounds, are, in in principle, possible.[3] The applied model allows, in principle, the calculation of the concentration of all 12 intrinsic defects as a function of the composition and temperature. In addition, the concentration of the defects in their different charge states and the electron and hole concentrations can be obtained. The results of these calculations are described in detail in Sec. V.

Irradiation-induced defects play an important role in the degradation of thin-film solar cells in space. The underlying damage formation mechanisms were reviewed for several solar cell materials by Woodyard.[4]

The positron annihilation spectroscopy, a well-established method to study vacancylike defects in solids, can yield valuable information on the structure of vacancies. Positrons may be trapped in open-volume defects and change their annihilation parameters specifically.[5] Because of their charge, positrons are sensitive to different charge states of a vacancy in semiconductors, and thus, they represent a selective tool for their identification. First applications of positron annihilation to the investigation of open-volume defects in CIS were recently published.[6,7] These results were obtained in epitaxially grown layers by the slow positron beam technique and are, thus, not directly comparable to the presented positron lifetime measurements in bulk material. To the best of our knowledge, there exist no further positron lifetime values in the literature up to now.

Monovacancies, or at most divacancies, can be produced by irradiation with 0.5–3 MeV electrons in crystals. This treatment was applied to $CuInSe_2$, and the formation and annealing behavior of vacancylike defects was investigated. Additionally to vacancies, electron irradiation produces, for example, negative ions (negatively charged nonopen volume defects) in crystals.[8,9] These negative ions act as shallow traps for positrons in semiconductors.[10]

In the following section, we summarize the material and experimental details. Section III gives a short introduction to the method of positron lifetime spectroscopy and its specific features used to study vacancy defects in semiconductors. In Secs. IV and V, we describe the results of calculations of positron lifetimes in bulk material and in defects and the defect chemistry in $CuInSe_2$. In Sec. VI, the results obtained by positron annihilation in as-grown and irradiated $CuInSe_2$ will be presented and also discussed. Conclusions are drawn in Sec. VII.

II. MATERIAL AND EXPERIMENTAL PROCEDURES

Bulk crystals of $CuInSe_2$ were grown by the Bridgman method. The samples of this material available to us were first studied by positron lifetime spectroscopy. Different re-

[a]Electronic mail: e3okz@mlucom.urz.uni-halle.de

sults were obtained, i.e., there were samples showing different average positron lifetimes in dependence on their compositions. However, these interesting results are not the subject of this paper. We rather chose a sample exhibiting a single component spectrum with the lowest average positron lifetime measured, i.e., showing no positron trapping (see discussion in Sec. VI A). From this result, we concluded that no lattice defects were detectable in this sample by positrons. We favored this sample for the electron irradiation experiment, since the absence of detectable defects prior to the irradiation allows the almost undisturbed study of irradiation-induced defects.

The Cu/In/Se composition of this sample was determined by microprobe measurements to be 0.3/0.18/0.52 after completion of irradiation and annealing experiments. This is a relatively large deviation from the stoichiometric point leading to the occurrence of at least one second phase. This is a typical problem of those ternary compounds. The positron source is large compared to the dimensions of second-phase inclusions. Hence, the measured positron lifetime is an average value of the lifetimes of the different phases. It is composed from the defect-related lifetimes in the occurring phases weighted by their corresponding volume fractions. Since the $CuInSe_2$ phase dominates, we assume that the detected irradiation-induced defects are typical for this phase.

Electron irradiation was performed at 4 K with a Van der Graaff accelerator in the Forschungszentrum Jülich. The incident energy of electrons was 2 MeV, and a fluence of 10^{18} cm^{-2} was applied for irradiation. The irradiated samples were mounted under liquid nitrogen in a cryoheater system to prevent warming up and annealing. Thereafter, an isochronal annealing (15 min) was performed in the range between 90 and 580 K. Temperature-dependent measurements after different annealing steps were carried out starting at 15 K.

The positron lifetimes were measured by using a fast–fast coincidence system having a time resolution of 260 ps. A pair of identical samples (two halves of the original sample) was sandwiched with the positron source consisting of radioactive $^{22}NaCl$ (0.5 MBq) covered with two thin (1 mg/cm^2) Al foils. The lifetime spectra consisting of about 5×10^6 annihilation events were analyzed after source and background corrections[11,12] with the trapping model.[13,14]

Hall-effect measurements were performed according to Van der Pauw.[15] The sample under investigation was found to be in the p-type conductivity state prior and after irradiation. Thus, the Fermi level was located close to or within the valence band.

III. POSITRON TRAPPING IN DEFECTS

Positrons are obtained by the β^+ decay of ^{22}Na. Their lifetime can be determined by detecting the time difference between the birth gamma (1.27 MeV gamma of β^+ decay) and the annihilation gamma (0.51 MeV). The lifetime spectrum consists of a sum of exponential decay components with the lifetimes τ_i and their intensities I_i. Positrons annihilate from the delocalized ground state in a perfect crystal. A single positron lifetime will be measured, $\tau=\tau_b$ (b: bulk). In the presence of defects of a distinct type, positrons may get localized at them and annihilate with a second lifetime $\tau_2=\tau_d$ (d: defect). This lifetime is larger than τ_b for open-volume defects, such as vacancies, due to the decrease in the electron density of the defect compared to the bulk. The lifetime spectrum consists, then, of two components. The positron trapping rate at defects, κ, may be determined from the experimentally obtained average positron lifetime $\overline{\tau}=I_1\tau_1+I_2\tau_2$ (with $\tau_2=\tau_d$) according to Eq. (1). The positron trapping rate κ is proportional to the defect concentration C_d. The proportional constant μ is the trapping coefficient, and must be obtained at least once by an independent reference method,

$$C_d=\frac{\kappa}{\mu}=\frac{1}{\mu\cdot\tau_b}\,\frac{\overline{\tau}-\tau_b}{\tau_d-\overline{\tau}}. \tag{1}$$

Semiconductor defects can exist in different charge states, depending on the position of the Fermi level in the energy band gap. A negative or positive charge state gives rise to additional Coulombic tails of the potential. Hence, positively charged vacancies are repulsive for positrons. The positron trapping in neutral vacancy defects is distinct, and moreover, the trapping is strongly enhanced in negative vacancies at low temperatures. The positron trapping at neutral vacancies is assumed to be temperature independent. The trapping coefficient μ depends on the defect type, defect charge, and possibly on temperature. Values for negative vacancies are $\mu=1-4\times10^{15}$ s^{-1} at 300 K (Refs. 16 and 17) and $\mu=10^{16}-10^{17}$ s^{-1} at 20 K.[17,18] μ is assumed to be about $10^{14}-10^{15}$ s^{-1} for neutral vacancies.[19]

Additionally, so-called shallow positron traps are possible candidates for positron trapping. They are negatively charged non-open-volume defects (negative ions), which are able to localize positrons in extended Rydberg states at low temperatures.[8,10] The positron lifetime in shallow traps is close to that in the bulk due to the negligible changes of the electron density felt by the positron. Therefore, as a result of competition between positron trapping in vacancies and in shallow traps, only the temperature dependence of the positron lifetime proves the presence of these shallow positron traps. The decomposition of the spectra is specially difficult at low temperatures due to this competitive trapping centers.

This temperature dependence of trapping in extended Rydberg states can be described[20] by

$$\kappa_{\mathrm{st}}=\kappa_{\mathrm{st0}}T^{-1/2}=\mu_{\mathrm{st0}}\,\frac{C_{\mathrm{st}}}{N}\,T^{-1/2}. \tag{2}$$

N is the number of atoms per cm^3, C_{st} (st: shallow trap) corresponds to the defect concentration, and μ_{st0} and κ_{st0} are the trapping coefficient and trapping rate, respectively, at 20 K. The trapping coefficient of negative ions in electron irradiated GaAs was determined to be $(5\pm2)\times10^{16}(T/\mathrm{K})^{-1/2}$ s^{-1}.[21] To simplify the model, only one effective Rydberg state was supposed instead of the complete Rydberg series.

The thermal detrapping from the shallow potential becomes dominant at higher temperatures, i.e., above 300 K, and almost no significant influence on the positron trapping is detectable. The temperature dependence of the detrapping rate δ from Rydberg states is given by

$$\delta = \frac{\mu_{st0}}{N}\left(\frac{m^* k_B T}{2\pi\hbar^2}\right)^{3/2} e^{-E_b/k_B T}. \quad (3)$$

E_b is the binding energy of positrons to the shallow trap, k_B the Boltzmann constant, and m^* the positron effective mass.

It should be noted that it is hardly possible to distinguish an isolated vacancy from a larger complex containing a vacancy by means of positron annihilation. Therefore, we cannot exclude that a detected vacancy is part of a defect complex.

IV. THEORETICAL CALCULATIONS OF POSITRON LIFETIMES

We used the superimposed-atom model by Puska and Nieminen[22] to calculate the positron lifetimes in the perfect lattice as well as in different defects in $CuInSe_2$. The calculations are described in detail elsewhere.[23] $CuInSe_2$ crystallizes in the chalcopyrite system. The copper and indium atoms occupy the corners and faces of the unit cell of this modified zinc-blende structure, while the selenium atoms replace the sulfur atoms in the zinc-blende structure. The number of unit cells (in defect calculations) and grid points was increased until the calculated lifetimes did not change anymore, by this we exclude the effects of the finite supercell size and of the discretization necessary for the numerical calculations, respectively.

We took for the calculations the low-frequency value ϵ_0 as well as an estimated value due to the lack of data on the high-frequency dielectric constant ϵ_∞ (lowering the high-frequency dielectric constant analogously to the known ratio for GaAs, CdTe,...) and one of even lower and higher value. This is to demonstrate that the deviations are systematically due to a change in ϵ. Larger dielectric constants are known to decrease the calculated lifetime values.[23]

The lifetimes calculated with the superimposed-atom model are always 5–7 ps lower than the corresponding experimental results.[20] Here, we find the experimental bulk lifetime in the same range in comparison to the theoretical data when using the estimated value for $\epsilon_\infty = 11.0$. The theoretical data can, thus, be scaled to the experimental bulk value as shown in the last column in Table I.

We have considered several types of vacancies in the lattice. The results are given in Table I. The lattice relaxation around the defects is not taken into account (see the discussion in Ref. 23). Note that the presented results are obtained with a non-self-consistent calculation method (see Ref. 23 for a discussion of the differences in self-consistent and non-self-consistent calculations).

As we can see from Table I, the lifetimes for different monovacancies are very close to each other, so that experimentally no distinction will be possible with a lifetime spectrometer. This is reflected in the very similar contour plots of the position probability density of the positron. Hence, we show only one example, the In vacancy. Here, we can see that, in comparison to the bulk, the positron wave function is localized at the site of the vacancy.

The calculated lifetimes are very close to each other (see Table I) for V_{CuSe} and V_{InSe}, considering all three possible combinations of nearest-neighbor divacancies. Thus, the contour plots look very similar, while V_{CuIn} leads to a significantly shorter lifetime, which is only slightly larger than the monovacancy lifetimes (see Table I). Comparing Figs. 1(c) and 1(d), it can be assumed that this is due to a larger separation of missing atoms. Hence, the positron feels effectively two separated vacancies and its lifetime is close to that of a monovacancy. In comparison, we see that in a trivacancy the positron is more localized in a region of low electron density, leading to an even longer lifetime.

TABLE I. Calculated positron lifetimes in the bulk and in vacancy defects of $CuInSe_2$. We used different values for the dielectric constant to demonstrate the change of the lifetimes since the exact high-frequency value is not known. The best estimate for $\epsilon_\infty = 11.0$ is given. The charge of the vacancies was not considered in the theoretical calculations. The calculated lifetimes were scaled to the experimentally determined bulk value $\tau_b = 235$ ps (last column) using the best estimate for $\epsilon = \epsilon_\infty = 11.0$. The scaling is to provide a better comparability to the experimental data. The lifetimes for monovacancies are very similar, indicating nearly the same electron densities where the positron is localized. Concerning the divacancies, the CuIn divacancy leads to a lower lifetime since the missing atoms are closer together.

τ(ps)	$\epsilon = 6.0$	$\epsilon = \epsilon_0 = 13.6$	$\epsilon = 20$	$\epsilon = \epsilon_\infty = 11.0$	$\epsilon = \epsilon_\infty = 11.0$ scaled
Bulk	235	226	224	228	235
V_{Cu}	251	241	238	243	250
V_{In}	258	247	244	249	257
V_{Se}	254	243	241	245	253
V_{CuIn}	275	262	259	264	272
V_{CuSe}	304	289	285	292	301
V_{InSe}	310	295	291	298	307
V_{CuInSe}	342	323	319	326	336

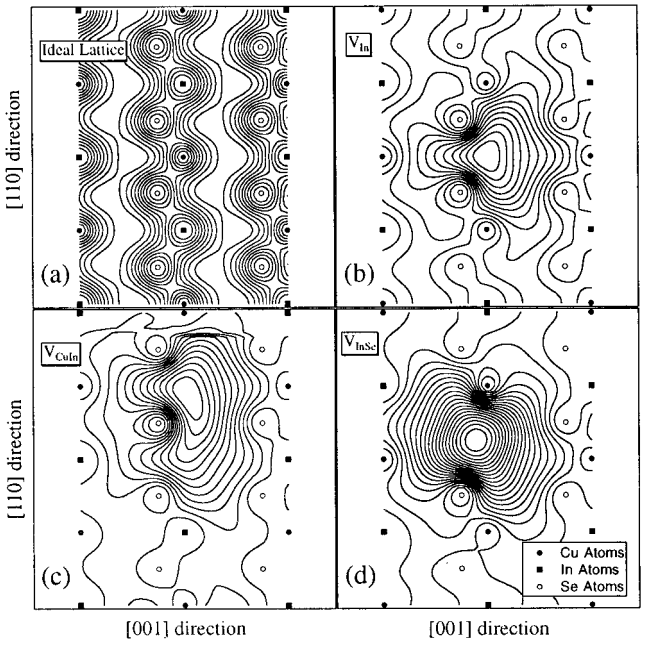

FIG. 1. Positron position probability density in the ideal lattice (a), in the In monovacancy (b), in the CuIn (c), and in the InSe divacancy (d) in $CuInSe_2$. The symbols mark the atomic positions in the 110 plane. The contour spacing is 1/10 of the maximum value for (a), 1/12 for (b), and 1/20 for (c) and (d).

TABLE II. Calculated formation enthalpies (in eV) of intrinsic defects in $CuInSe_2$. A formation entropy $\Delta S = 3k_B$ was assumed for all defects.

Defect	$V_{Cu}^{0/-}$	$V_{In}^{0/-}$	$V_{Se}^{0/+}$	$Cu_i^{0/+}$	$In_i^{0/+}$	$Se_i^{0/-}$
Formation enthalpy[a]	3.2	2.4	2.6[c]	⋯	⋯	⋯
Formation enthalpy[b]	2.6	2.4	2.8	4.4	9.1	22.4
Defect	$Cu_{In}^{0/-}$	$In_{Cu}^{0/+}$	$Cu_{Se}^{0/-}$	$In_{Se}^{0/-}$	$Se_{Cu}^{0/+}$	$Se_{In}^{0/+}$
Formation enthalpy[a]	1.9	1.6	5.4	5.0	6.0	5.2
Formation enthalpy[b]	1.5	1.4	7.5	5.0	7.1	5.5

[a]Reference 24.
[b]Reference 25.
[c]The value was printed incorrectly in Ref. 24.

V. DEFECT CHEMISTRY IN CIS

The concentration of the dominating defects can be estimated by means of defect chemistry. Some results are available for $CuInSe_2$ in thermodynamical equilibrium.[24,25] The usual approach to solve the problem is based on Kröger's general ideas of the defect chemistry of ionic crystals. They give the theoretical background for these calculations on the basis of suitable thermodynamic variables such as the partial gas pressure or the thermodynamic activity of one of the components.[26–28] These ideas have been extended to ternary ionic compounds by Groenink and Janse[29] under the assumption that anion–cation antisite defects can be neglected. These defects cannot be ruled out *a priori* in ternary semiconductors with mixed covalent and ionic bonding. Therefore, an extension of the model that allows the direct calculation of the concentrations of all intrinsic defects has been developed by one of the authors.[3] It requires the knowledge of the formation enthalpies and entropies, and the electronic levels of all 12 intrinsic defects.

Direct measurements of formation enthalpies and entropies of intrinsic defects of CIS have not yet been available because of the complexity of the defect chemistry. Therefore, one has to rely on indirect conclusions and theoretical estimates. Two approximate calculations of the formation energies of intrinsic defects have been carried out for $CuInSe_2$.[24,25] They are summarized in Table II. Although there are some discrepancies in the absolute values, the results show an agreement that there are only six defects, which have formation energies below 5 eV. In addition, one has to consider that the defects can occur in different charge states. The numerical results of the defect concentrations are presented as functions of the composition in a defect diagram, which shows the majority defects for a given range of compositions (Fig. 2). One also obtains the free-carrier concentration based on the electronic levels of the majority defects. It could be shown that one can obtain a good agreement between the calculations and the observed *p*- or *n*-type behavior. Typically, the deviations in the copper, indium, or selenium concentrations are at least 1 at. %. Therefore, stoichiometries close to the ideal composition are not considered here (white area in Fig. 2).

Summarizing all results, one obtains that out of the 12 possible defects, only seven are relevant, the vacancies V_{Cu}, V_{In}, V_{Se}, the cation–cation antisites Cu_{In}, In_{Cu}, and the anion–cation antisites Cu_{Se}, In_{Se}. The remaining five defects, in particular, all interstitial defects, occur at concentrations that are orders of magnitudes lower compared to the dominant defect concentrations. Four different regimes for large deviations (>1at. %) from the ideal stoichiometry have to be considered with the majority defects given in Fig. 2.

The charge states of the different defects are of essential importance with respect to positron trapping. A schematic presentation of the electrical behavior of the above mentioned dominating vacancies and antisite defects is shown in Fig. 3. The scheme was drawn according to Refs. 24 and 25.

There are several experimental results showing the existence of such ionization levels in the band gap of $CuInSe_2$. A number of shallow levels have been measured and tentatively related to some of the majority defects.[27,30] A level at 70 meV above the valence-band edge was attributed to the acceptor-type vacancy $V_{Cu}^{0/-}$. Further acceptor-type levels

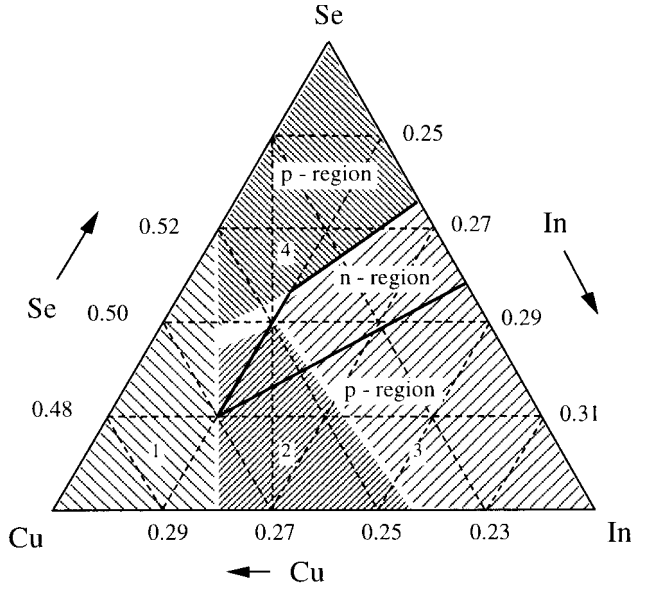

FIG. 2. Majority defects depicted in a ternary diagram of Cu, In, and Se for larger deviations from ideal stoichiometry. There are four regions characterized by the dominating defects: (1) Cu_{Se}^{2+}, Cu_{In}^{2-}, (2) V_{Se}^{2+}, In_{Se}^{2-}, Cu_{Se}^{2-}, (3) In_{Cu}^{2+}, V_{Cu}^{-}, and (4) In_{Cu}^{2+}, V_{In}^{2-}, V_{Cu}^{-}. The composition range bounded by solid lines shows *n*-type conductivity.

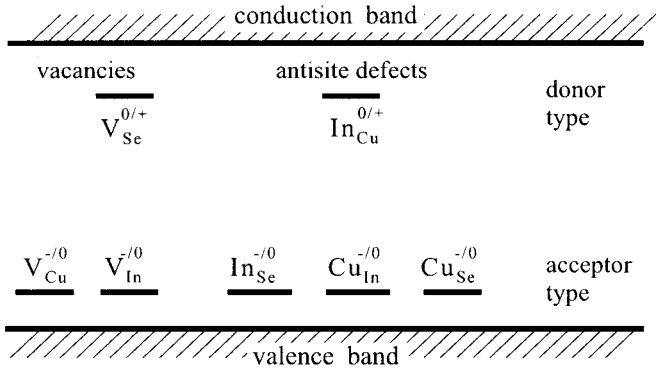

FIG. 3. Schematic presentation of the ionization levels in the band gap of the dominating defects, i.e., the vacancies and four of six possible antisite defects in $CuInSe_2$ according to Refs. 24 and 25.

were found at 50 and 80 meV (assigned to $V_{In}^{0/-}$) and at 50 and 100 meV ($Cu_{In}^{0/-}$). Donor-type defects were found at 60 and 80 meV ($V_{Se}^{0/+}$) and at 20 and 50 meV ($In_{Cu}^{0/+}$) below the conduction-band edge, respectively.

Since the sample is proved to be of p-type conductivity prior to and after electron irradiation, positron annihilation is restricted to the detection of Cu and In vacancies.

It is known that negatively charged antisite defects may act as shallow positron traps at low temperatures.[10] It can be concluded from Fig. 3 that In_{Se}^{-}, Cu_{In}^{-}, and Cu_{Se}^{-} are possible candidates for these shallow traps in p-type material.

VI. RESULTS AND DISCUSSION

A. As-grown material

The composition of the investigated specimen (Cu 30 at. %, In 18 at. %, and Se 52 at. %) leads to p-type conductivity and belongs to region 1 in Fig. 2 with the majority defects Cu_{Se}^{2+} and Cu_{In}^{2-}. It is expected that the concentration of any vacancy-type defect is orders of magnitudes lower than the concentration of these antisite defects. This is in agreement with the positron lifetime measurements of the as-grown sample, where an average positron lifetime of 235.2 ps has been measured. Since we have detected a one-component spectrum with the lowest lifetime ever observed in our $CuInSe_2$ samples, we conclude that this is the positron lifetime in bulk material. This means that the concentration of neutral and negatively charged vacancies is smaller than about 5×10^{15} cm^{-3}.[17] The experimentally determined value is slightly higher in comparison with the calculated value of 228 ps (see Table I). This difference is typical for such a type of calculations using the superimposed-atom model and is also found in other semiconductors.[20] This discrepancy between the calculated and experimentally determined positron lifetimes is usually taken into account by a scaling factor (last column in Table I).

B. Defects after electron irradiation

An increase in the average lifetime of about 30 ps indicates the presence of a high density of open-volume defects in the as-irradiated state (2 MeV electron energy, dose of

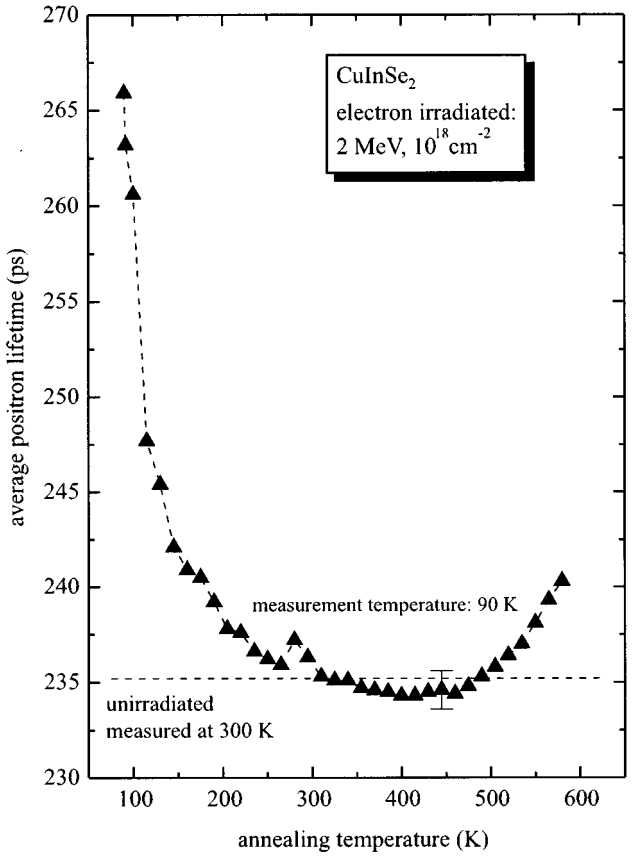

FIG. 4. Average positron lifetime as a function of annealing temperature in electron irradiated ($E=2$ MeV, $\Phi=10^{18}$ cm^{-2}, $T=4$ K) $CuInSe_2$ measured at 90 K.

10^{18} cm^{-2}). A decomposition of the spectra is not possible in the annealing range between 90 and 250 K and at the measurement temperature of 90 K. This is in accordance with the observations in electron-irradiated III–V compounds,[31,9] and it is due to the competitive trapping of positrons in shallow positron traps as well as in vacancylike defects (see the discussion below). The average positron lifetime of about 260 ps indicates the presence of open-volume defects larger than monovacancies, i.e., most probably divacancies. Although no decomposition of the spectra is possible, this conclusion can be drawn, since the average lifetime exceeds the calculated value of monovacancies, which is 257 ps at maximum (see Table I).

Figure 4 shows the annealing behavior of irradiated $CuInSe_2$, reflected in a sharp decrease in the average positron lifetime in the range between the temperature of sample installation (90 K) and 250 K.

As explained above, we conclude that divacancies detectable by positrons disappear in the main annealing stage. It is not possible to distinguish between several kinds of divacancies because there is no information so far about ionization levels, charge states, and dominating kind of divacancies.

The determination of defect introduction rates of the electron irradiation is rather complicated due to the lacking spectra decomposition at low temperatures. The reason is the

competitive trapping between shallow traps and open-volume defects and its complex temperature dependence. Thus, the attempt of determining the vacancy-defect introduction rate yields only a lower-limit estimation. We used the average lifetime obtained at 90 K after irradiation and transfer of the sample to the cryoheater system, $\overline{\tau}=266$ ps. The defect-related lifetime for divacancies is used in order to determine the positron trapping rate κ (see the discussion above). This value is taken as the average over the three theoretically calculated divacancy lifetimes, $\tau_2=293$ ps. κ was obtained according to Eq. (1), $\kappa=4.7\times10^9\ \mathrm{s}^{-1}$. The influence of shallow traps on this calculation of κ is ignored, leading to a too low trapping rate of divacancies. Therefore, only a lower-limit estimation for their concentration is obtained. Using a trapping coefficient of $\mu=1\times10^{16}\ \mathrm{s}^{-1}$, it is determined to be $C_d>2\times10^{16}\ \mathrm{cm}^{-3}$. We use this rather high value of μ to stay in the framework of the lower-limit estimation of the introduction rate of this defect. It should be noted that the trapping coefficient could be one order of magnitude smaller when neutral divacancies dominate the positron trapping. The introduction rate is calculated as the quotient of the divacancy concentration and the electron dose to be $>0.02\ \mathrm{cm}^{-1}$ for a low-temperature irradiation. The conceivable annealing processes between the irradiation temperature and 90 K were neglected.

This lower-limit estimation of the introduction rate is comparable to other elemental and compound semiconductors. A value of 0.03 and $0.3\ \mathrm{cm}^{-1}$ was reported for low-temperature electron irradiation of p- and n-type Si, respectively.[32] An introduction rate of about $1\ \mathrm{cm}^{-1}$ was given for electron-irradiated GaAs ($T_{\mathrm{irr}}=4$ K).[33] The total introduction rate can, nevertheless, reach a very high value; $\approx7\ \mathrm{cm}^{-1}$ was found for GaAs in one sublattice.[33] The defect concentration of shallow traps (see the discussion below) suggests also a higher total introduction rate for CIS.

The positron lifetime reaches 235 ps, i.e., the positron bulk lifetime after annealing at about 250 K and at a measurement temperature of 90 K. This experimental result can be explained either by the decrease in the concentration of open-volume defects below the sensitivity limit of positron annihilation, or by the fact that possibly existing vacancy-type defects are positively charged. A further possibility would be the existence of shallow positron traps, which are completely dominating the positron trapping. The latter case can be excluded by temperature-dependent positron lifetime measurements, since the shallow traps should lose their trapping efficiency at high temperatures (see Sec. III). The result of corresponding experiments performed after annealing at 265 and 340 K is shown in Fig. 5. Only a slight increase in the average positron lifetime was observed, indicating that only the first two explanations given above have to be taken into account. Hence, we conclude that no neutral or negatively charged open-volume defects are present in a considerable amount in the annealing temperature range between 250 and 400 K.

A further increase in the average lifetime is detectable above 450 K (see Fig. 4). Obviously, a new defect type is formed in this annealing range. A possible cause could be the evaporation of one of the components of the ternary compound, and consequently, the formation of vacancies in the respective sublattice. However, this possibility is unlikely at this low temperature. An annealing experiment of a reference sample proved this assumption.

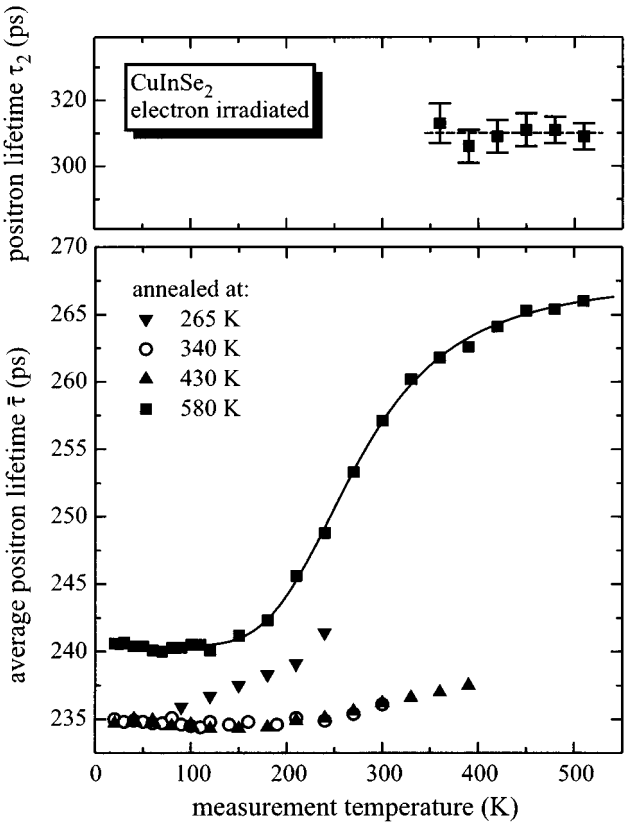

FIG. 5. The lower panel shows the average positron lifetime as a function of measurement temperature in electron-irradiated ($E=2$ MeV, $\Phi=10^{18}\ \mathrm{cm}^{-2}$, $T=4$ K) $CuInSe_2$ after different annealing steps. The fitted curve (solid line) corresponds to the two-defect trapping model and is drawn for the state after the 580 K annealing step. The upper panel shows the defect-related lifetime obtained as a result of the two-component spectra decomposition after annealing at 580 K. The spectra decomposition could only be performed at higher temperatures due to competitive trapping by shallow traps in the low-temperature range.

A very pronounced increase in the average lifetime at high measurement temperatures was found at an annealing temperature of 580 K (Fig. 5). The temperature dependence of the positron trapping in this annealing state is very distinct. The upper part of Fig. 5 shows the defect-related positron lifetime obtained as a result of the spectra decomposition of temperature-dependent measurements as (310 ± 5) ps. It could be determined only in the temperature range above 350 K. The decomposition was difficult below this temperature due to the simultaneous trapping in shallow positron traps.

The divacancy concentration can be calculated due to the spectra decomposition. A defect concentration of $C_d=1.3\times10^{17}\ \mathrm{cm}^{-3}$ was determined according to Eq. (1) at a measurement temperature of 500 K after annealing at 580 K. We used a trapping coefficient of $1\times10^{15}\ \mathrm{s}^{-1}$.[17] It is concluded from the defect-related lifetime of 310 ps, in comparison to the calculated lifetimes in Table I, that divacancies are

detected. It is known that Cu and In atoms become mobile at an annealing temperature of about 570 K ($D_{Cu}=1.8\times10^{-8}$ cm^2 s^{-1}, $D_{In}=1.4\times10^{-8}$ cm^2 s^{-1}).[34,35] The diffusion coefficient of Se atoms is comparably very small ($D_{Se}<1\times10^{-12}$ cm^2 s^{-1}) at this temperature.[36]

We assume that this defect type is created during annealing above 450 K due to a defect reaction of irradiation-induced defects invisible for positions. Obviously, the primary annealing stage up to 250 K does not lead to a complete annealing of the radiation defects. Part of the defects survives the annealing stage that is completed below 250 K as defects invisible for positrons. Possible candidates are defects or defect complexes containing no vacancies. In the case that vacancies are part of the complex, it must be concluded that the complex, or at least the vacancy, is positively charged. Therefore, one has to conclude that at least three different defect types are involved in the annealing behavior up to 600 K.

In order to confirm that this ''invisible'' defect is caused by the irradiation, an annealing experiment was performed with an unirradiated reference sample. No change of the average positron lifetime was observed during an annealing up to 1000 K.

Fits according to the trapping model were applied to the temperature-dependent positron lifetime measurements after annealing at 580 K. Positron trapping in and detrapping from shallow traps corresponding to Eqs. (2) and (3), as well as direct trapping in neutral vacancies, were taken into account in the trapping model. There are four fitting parameters: the trapping coefficient for the shallow traps μ_{st0}, the binding energy E_b of the positrons to the shallow traps, the concentration of shallow traps C_{st}, and the trapping rate of direct trapping in vacancies κ_V. The model is complex and the parameters are partly dependent on each other. Therefore, the results of the fitting procedure should not be overestimated. In all figures presented in this paper, dashed lines are only to guide the eye, while solid lines correspond to fits.

The fit yields the following results: the binding energy of positrons to shallow traps, $E_b=(88\pm5)$ meV, the trapping coefficient for the shallow traps at 20 K, $\mu_{st0}=(1.4\pm0.4)\times10^{17}$ s^{-1}, the concentration of shallow traps, $C_{st}=(1.5\pm0.4)\times10^{18}$ cm^{-3}, and the trapping rate of trapping in divacancies, $\kappa_V=(1.6\pm0.1)\times10^{10}$ s^{-1}. The latter value corresponds to a divacancy concentration of $(6.6\pm0.4)\times10^{17}$ cm^{-3}. The discrepancy between this value and the value obtained according to Eq. (1) (compare the discussion above) can be explained by the small but still existing influence of shallow traps even in the temperature range above 400 K. This can be seen from the slight increase in the average positron lifetime in this temperature range.

The errors given in the last paragraph are the statistical errors found as results of the fits. It should be noted that the real confidence range is larger due to the mutual statistical dependency of the parameters. However, the accuracy is still better than half an order of magnitude. The obtained values are comparable to values obtained in other electron irradiated compounds. The positron binding energy of the shallow traps can directly be compared, whereas the defect concentrations are directly linked to the actual irradiation conditions. The values of 90, 65, and 120 meV found in GaAs:Zn, GaAs:Te,[37] and InP,[9] respectively, are similar to the value found in CIS.

As mentioned above, the Cu_{In}^{2-} antisite defect is one of the major defects, and it should represent the dominating acceptor. Thus, this defect is the most probable candidate for the observed shallow positron trap. However, no closer identification is possible with the applied experimental techniques.

The fact that the divacancy concentration obtained after 580 K annealing is above the value estimated for the divacancy concentration in the as-irradiated state is, at a first glance, surprising. There is no contradiction between these values since the value obtained at 90 K represents only a lower-limit estimation. Obviously, a large number of shallow traps influences strongly the estimation of the divacancy concentration at low temperatures.

Since the charge state of the divacancy is unknown, we attempted to fit the positron lifetime taking into account a negatively charged open-volume defect. The resulting curve is identical with that of the other model (neutral divacancy), and the obtained quantities are also physically reasonable. Therefore, we cannot distinguish between neutral or negatively charged divacancies by our temperature-dependent experiments. Positively charged defects are expected to repel positrons and they should, thus, be no positron traps.

VII. CONCLUSIONS

$CuInSe_2$ was studied after low-temperature (4 K) 2 MeV electron irradiation. No positron trapping was observed for the unirradiated sample, indicating that the concentration of neutral and negatively charged vacancies is smaller than 5×10^{15} cm^{-3}. The positron bulk lifetime was determined to be 235 ps.

An increased average positron lifetime indicates the appearance of divacancy-type defects after the first annealing step during assembling the irradiated sample into the cryostat. A lower-limit estimation of their introduction rate yields a value of 0.02 cm^{-1}. The average positron lifetime reaches the bulk value during the annealing treatment up to 250 K and increases again at annealing temperatures above 450 K. It is concluded that defect complexes undetectable by positrons exist in the temperature range between 250 and 450 K. These are most probably complexes without vacancies or positively charged defect complexes containing vacancies. They undergo above 450 K a further defect reaction leading to a divacancy signal of thermally more stable complexes. Obviously, new neutral or negatively charged divacancy defects are created with a concentration of about 1×10^{17} cm^{-3}.

A large number of shallow positron traps was detected after electron irradiation. Thus, further irradiation-induced defects exist in addition to the observed vacancy defects, which are negatively charged and exhibit no open volume. The Cu_{In}^{2-} antisite defect is the dominating acceptor in the investigated material according to a simple defect-chemical approach,[24] and may be responsible for the positron trapping in these shallow positron traps.

The positron bulk lifetime, as well as the defect-related lifetimes for mono-, di-, and trivacancies, were theoretically calculated according to the superimposed-atom model by Puska and Nieminen.[22]

ACKNOWLEDGMENTS

Dr. F. Dworschak from Forschungszentrum Jülich is kindly acknowledged for carrying out the electron irradiations. The authors thank Professor D. Cahen (Weizmann Institute of Science, Israel) for his valuable discussion. The studies are supported by the German–Israeli Foundation for Scientific Research and Development, the Deutsche Forschungsgemeinschaft, and the Vereinigung der Freunde und Förderer der Martin-Luther-Universität Halle-Wittenberg e.V.

[1] H. W. Schock, in *12th European Photovoltaic Solar Energy Conference*, edited by R. Hill (H. S. Stephans, Bedford, England, 1994), p. 994.
[2] M. Yamaguchi, J. Appl. Phys. **78**, 1476 (1995).
[3] J. E. Kluin and H. J. Möller, in *11th European Photovoltaic Solar Energy Conference* (Harwood Academic, Switzerland, 1993), p. 858.
[4] J. R. Woodyard, Sol. Cells **31**, 297 (1991).
[5] P. Hautojärvi, in of *Topics in Current Physics*, Vol. 12, edited by P. Hautojärvi (Springer, Berlin, 1979).
[6] A. J. Nelson, A. M. Gabor, J. R. T. M. A. Contreras, R. Noufi, P. E. Sobol, P. Asoka-Kumar, and K. G. Lynn, J. Appl. Phys. **78**, 269 (1995).
[7] A. J. Nelson, A. M. Gabor, M. A. Contreras, A. Mason, P. Asoka-Kumar, and K. G. Lynn, Sol. Energy Mater. Sol. Cells **41**, 315 (1996).
[8] C. Corbel, F. Pierre, P. Hautojärvi, K. Saarinen, and P. Moser, Phys. Rev. B **45**, 3386 (1992).
[9] A. Polity and T. Engelbrecht, Phys. Rev. B **55**, 10 480 (1997).
[10] K. Saarinen, P. Hautojärvi, A. Vehanen, R. Krause, and G. Dlubek, Phys. Rev. B **39**, 5287 (1989).
[11] B. Somieski, T. E. M. Staab, and R. Krause-Rehberg, Nucl. Instrum. Methods Phys. Res. A **381**, 128 (1996).
[12] T. E. M. Staab, B. Somieski, and R. Krause-Rehberg, Nucl. Instrum. Methods Phys. Res. A **381**, 141 (1996).
[13] M. Bertolocciani, A. Bisi, G. Gambarini, and L. Zappa, Phys. Rev. C **4**, 734 (1971).
[14] W. Brandt, Appl. Phys. **5**, 1 (1974).
[15] L. J. Van der Pauw, Philips Res. Rep. **13**, 1 (1958).
[16] R. Krause-Rehberg, A. Polity, and T. Abgarjan, Mater. Sci. Forum **175-178**, 427 (1995).
[17] R. Krause-Rehberg and H. Leipner, Appl. Phys. A: Solids Surf. **64**, 457 (1997).
[18] P. Hautojärvi, Mater. Sci. Forum **175-178**, 47 (1995).
[19] M. J. Puska, J. Phys.: Condens. Matter **1**, 7347 (1989).
[20] M. J. Puska and R. M. Nieminen, Rev. Mod. Phys. **66**, 841 (1994).
[21] K. Saarinen, A. P. Seitsonen, and P. Hautojärvi, Phys. Rev. B **52**, 10 932 (1995).
[22] M. J. Puska and R. M. Nieminen, J. Phys. F **13**, 333 (1983).
[23] F. Plazaola, A. P. Seitsonen, and M. J. Puska, J. Phys.: Condens. Matter **6**, 8809 (1994).
[24] H. J. Möller, Sol. Cells **31**, 77 (1990).
[25] H. Neumann, in *Verbindungshalbleiter*, edited by K. Unger and H. Schneider (Geest & Porting, Leipzig, 1986).
[26] F. A. Kröger, *The Chemistry of Imperfect Crystals* (North-Holland, Amsterdam, 1973).
[27] F. A. Kröger and H. J. Vink, Solid State Phys. **3**, 307 (1956).
[28] H. Schmalzried and C. Wagner, Z. Phys. Chem. Neue Folge **31**, 198 (1962).
[29] J. A. Groenink and P. H. Janse, Z. Phys. Chem. Neue Folge **110**, 17 (1978).
[30] G. Masse and E. Redjai, J. Phys. Chem. Solids **47**, 1 (1986).
[31] C. Corbel, F. Pierre, P. Hautojärvi, K. Saarinen, and P. Moser, Phys. Rev. B **41**, 10 632 (1990).
[32] G. D. Watkins, Mater. Sci. Technol. **4**, 105 (1992).
[33] D. Pons and J. C. Bourgoin, J. Appl. Phys. C: Solid State Phys. **18**, 3839 (1985).
[34] B. Tell and P. M. Bridenbaugh, J. Appl. Phys. **48**, 2477 (1977).
[35] J. Gonzales, C. Rincon, A. Reslonslo, and P. Negute, Jpn. J. Appl. Phys. **19**, 29 (1980).
[36] H. J. von Bardeleben, J. Appl. Phys. **56**, 321 (1984).
[37] A. Polity, F. Rudolf, C. Nagel, S. Eichler, and R. Krause-Rehberg, Phys. Rev. B **55**, 10 467 (1997).